BioGecko

Vol 12 Issue 03 2023

ISSN NO: 2230-5807

Numerical Based Study on the Flow Pattern of Casson Nano fluid under Thermo Diffusion in Conducting Field

M. Parvathi[1], P. Roja[2], P. Chandra Reddy[3*], M. Umamaheswar

[1,2,3*,4]*Department of Mathematics, Annamacharya Institute of Technology and Sciences (Autonomous) Rajampet -516126, A.P., India*

Corresponding Email: [3]chandramsc01@gmail.com*

Abstract

A numerical modeling has been done and examined to draw out the variations in the flow pattern of Casson nanofluid past a stretched porous sheet in conducting field. The governed non-linear partial differential equations are changed into ordinary form of differential equations by inserting related similarity transforms and then solved by Shooting technique using MAT lab. The results obtained are presented to explore the effects of various parameters through graphs and tables. It is noticed that both the velocities decreases with the increase in Casson parameter.

Keywords: MHD, 3D flow, Chemical reaction, Radiation, Soret effect, Dufour effect, Casson Nanofluid, Porous medium, Stretching sheet.

1. INTRODUCTION

The researchers are mainly concentrating on boosting up the heat transfer rate as well as thermal conductivity. In order to gain these results in the fluid flows, nanofluids came into existence. Nano fluid is the mixture of nano particles into base fluids like water, ethylene glycol and kerosene. The foremost analyses on this modeling were done by Choi [1, 2]. A detailed report on the flows nano fluids considering a variety of nano particles with different physical properties is found in these articles. Hamad [3] gave analytical solution for these flows over a stretched linear sheet. Khan et al. [4] added radiation and examined the flow over a stretched sheet in conducting field.The researchers further focused on nanofluid flows with magnetic field properties which is termed as magnetohydrodynamics. This is done based on the significance of these analyses in chemical industries, oil refinery process, underground water flows and also in petroleum industries. MHD is a key role in medical field in the process of physiology of human body like MRT, MRI and NMRI. Nayak et al. [5] considered and analyzed these flows with convection end conditions in 3- dimensional mode. Hayat et al. [6] discussed the cross-diffusion influences past an exponentially stretchable surface in porous medium. Sheikholeslami et al. [7] choosed and examined Lorentz force for copper-water nanofluid flow under heat transfer cavity. Aurang Zaib et al. [8] performed and solved numerically the second grade of Casson nano fluid past a wedge with binary reaction. Hayat et al. [9] revealed on shrinking surface viscous nanofluid

under slipped velocity and jumped temperature. Nayak et al. [10] reported on 3D nanofluid along a linearity stretching area.
The main aim of the present study is to investigate the flow pattern of Casson nanofluid in a conducing field in the presence of Dufour effect over a porous stretching sheet. The novel thing in this work is the inclusion of Casson parameter and diffusion- thermo effect for base work in the published paper.

Formulation of the problem:
A 3-dimensional mode of incompressible, naturally convective and also conducting nanofluid flow is considered and along a stretched permeable sheet. Assume a transverse magnetic field of uniform strength B_0 is applied parallel to the z-axis. A fluid which allows reducing the shear stress of the fluid and possesses infinite viscosity is termed as Casson fluid. This non-Newtonian fluid has non viscous nature at infinite shear rate. The inducted magnetism and impressible conducting field are unobserved by arrogating magnetic Reynolds number to be extensively miniature. The flow is taken along a stretching sheet which is a leaky one.

Based on these suppositions, the expressions that govern the flow nature (Nayak et al. [10]) are as follows:

$$\frac{\partial u}{\partial x}+\frac{\partial v}{\partial y}+\frac{\partial w}{\partial z}=0 \tag{1}$$

$$u\frac{\partial u}{\partial x}+v\frac{\partial u}{\partial y}+w\frac{\partial u}{\partial z}=\frac{1}{\rho_{nf}}\left\{\mu_{nf}\left(1+\frac{1}{\beta}\right)\frac{\partial^2 u}{\partial z^2}+(\rho\beta)_{nf}\,g(T-T_\infty)+(\rho\beta^*)_{nf}\,g(C-C_\infty)-\sigma B_0^2 u-\frac{\nu u}{k}\right\} \tag{2}$$

$$u\frac{\partial v}{\partial x}+v\frac{\partial v}{\partial y}+w\frac{\partial v}{\partial z}=\frac{1}{\rho_{nf}}\left\{\mu_{nf}\left(1+\frac{1}{\beta}\right)\frac{\partial^2 v}{\partial z^2}+(\rho\beta)_{nf}\,g(T-T_\infty)-(\rho\beta^*)_{nf}\,g(C-C_\infty)-\sigma B_0^2 v+\frac{\nu w}{k}\right\} \tag{3}$$

$$u\frac{\partial T}{\partial x}+v\frac{\partial T}{\partial y}+w\frac{\partial T}{\partial z}=\frac{k_{nf}}{(\rho C_p)_{nf}}\frac{\partial^2 T}{\partial z^2}-\frac{1}{(\rho C_p)_{nf}}\frac{\partial q_r}{\partial z}-Q(T-T_\infty)+Q_l(C-C_\infty)+\frac{D_B K_{nf}}{(\rho C_P)_{nf}}\frac{\partial^2 C}{\partial z^2} \tag{4}$$

$$u\frac{\partial C}{\partial x}+v\frac{\partial C}{\partial y}+w\frac{\partial C}{\partial z}=D_B\frac{\partial^2 C}{\partial z^2}+D_l\frac{\partial^2 T}{\partial z^2}-Kr^*(C-C_\infty) \tag{5}$$

subjeeted to the boundery conditions

$$u=U_w(x)=ax, v=V_w(x)=bx\ ,\ w=0,\ T=T_w,\ C=C_w \text{ at z=0}$$
$$u\to 0,\ v\to 0,\ w\to 0, T\to T_\infty,\ C\to C_\infty \quad \text{as } z\to\infty \tag{6}$$

where a & b are positive for stretchiing sheet.

The Rosselend approximaation, the radiative heat term is given by

$$q_r=\frac{-4\sigma^*}{3k^*}\frac{\partial T^4}{\partial z},\ T^4=4T_\infty^3 T-3T_\infty^4,\ \frac{\partial q_r}{\partial \bar{z}}=-16\frac{T_\infty^3\sigma^*}{3k^*}\frac{\partial^2 T}{\partial \bar{z}^2} \tag{7}$$

From (7), (8) in addition to eq. (4) the energy equation transforms is

$$u\frac{\partial T}{\partial x}+v\frac{\partial T}{\partial y}+w\frac{\partial T}{\partial z}=\frac{k_{nf}}{(\rho C_p)_{nf}}\frac{\partial^2 T}{\partial z^2}-\frac{16\sigma^* T_\infty^3}{(\rho Cp)_{nf}3k^*}\frac{\partial^2 T}{\partial z^2}-\frac{Q}{(\rho Cp)_{nf}}(T-T_\infty)+Q_l(C-C_\infty) \tag{8}$$

We consider the dimensionless variables as

$$u=axf'(\eta),\ v=ayf'(\eta),\quad w=-(a\nu_f)^{1/2}(f(\eta)+g(\eta)),\ \theta(\eta)=\frac{T-T_\infty}{T_w-T_\infty},\ C(\eta)=\frac{C-C_\infty}{C_w-C_\infty},\quad \eta=\left(\frac{a}{\nu_f}\right)^{1/2}z \tag{9}$$

By using (7)-(10) Eqs. (2),(3),(8) and (5)

$$\left(1+\frac{1}{\beta}\right)f'''+\varepsilon\left\{\varepsilon_1\left((f+g)f''-(f')^2\right)+\left(\varepsilon_2\gamma_1\theta+\varepsilon_4\gamma_2 C-M-kl\right)f'\right\}=0 \tag{10}$$

$$\left(1+\frac{1}{\beta}\right)g'''+\varepsilon\left\{\varepsilon_1\left((f+g)g''-(g')^2\right)-\left(\varepsilon_2\gamma_3\theta\varepsilon+\varepsilon_4\gamma_4 C+M-kl\right)g'\right\}=0 \tag{11}$$

$$(A+R)\theta''+\varepsilon_3\left(\Pr(f+g)\theta'+Q_l\right)-Q_H\theta+D_f C''=0 \tag{12}$$

$$C''+Sc(f+g)C'+S_0 Sc\theta''-ScKrC=0 \tag{13}$$

with the boundary conditions

$$f'(\eta)=1,\ g'(\eta)=\lambda,\ f(\eta)=0,\ g(\eta)=0,\quad \theta(\eta)=1,\ C(\eta)=1 \text{ at } \eta=0$$
$$f'(\eta)\to 0,\ g'(\eta)\to 0,\ \theta(\eta)\to 0,,\ C(\eta)\to 0 \qquad \text{as } \eta\to\infty \tag{14}$$

where $\varepsilon=(1-\phi)^{2.5}$, $\varepsilon_1=1-\phi+\phi\left(\frac{\rho_s}{\rho_f}\right)$, $\varepsilon_2=1-\phi+\phi\left(\frac{(\rho\beta)_s}{(\rho\beta)_f}\right)$, $\varepsilon_3=1-\phi+\phi\left(\frac{(\rho C_p)_s}{(\rho C_p)_f}\right)$,

$\varepsilon_4=1-\phi+\phi\left(\frac{(\rho\beta^*)_s}{(\rho\beta^*)_f}\right)$, $M=\frac{\sigma B_0^2}{a\rho_f}$, $R=\frac{16\sigma^* T_\infty^3}{3k^* k_f}$, $\lambda=\frac{b}{a}$,

$\gamma_1=\frac{g\beta_f(T_w-T_\infty)}{au}$, $\gamma_2=\frac{g\beta_f^*(C_w-C_\infty)}{au}$, $\gamma_3=\frac{g\beta_f(T_w-T_\infty)}{av}$,

$\gamma_4=\frac{g\beta_f^*(C_w-C_\infty)}{av}$, $kl=\frac{\nu_f}{ak\rho_f}$, $Q_H=\frac{Q}{a(\rho Cp)_f}$,

$Q_l=\frac{Q_l^*(C_w-C_\infty)}{a(T_w-T_\infty)}$, $Sc=\frac{\nu_f}{D_B}$, $S_0=\frac{D_l(T_w-T_\infty)}{\nu_f(C_w-C_\infty)}$, $Kr=\frac{Kr^*}{a}$, $\Pr=\frac{\nu_f}{\alpha_f}$, $A=\frac{k_{nf}}{k_f}$

In terms of dimensionless variables are given by the local skin friction co-efficient about x-axis C_{fx} and y-axis C_{fy}, local Nusselt number Nu_x and local Sherwood number Sh_x

$$\mathrm{Re}_x^{1/2}C_{fx}=\frac{1}{(1-\phi)^{2.5}}f'(0)\quad \mathrm{Re}_y^{1/2}C_{fy}=\frac{1}{\lambda^{3/2}(1-\phi)^{2.5}}g'(0)\quad \mathrm{Re}_x^{-1/2}Nu_x=-A(1+R)\theta'(0)\quad \mathrm{Re}_x^{-1/2}Sh_x=-(1+R)C'(0)$$

2. RESULTS (OUTCOMES) AND OBSERVATIONS

A numerical study has been performed to draw out the variations in the flow pattern of Casson nanofluid past a stretched porous sheet in conducting field. To analyze velocity, temperature and concentration profiles, the parameters like thermal radiation, heat generation, radiation

absorption, diffusion thermo effect, chemical reaction are also considered into account with the volume fraction $\phi = 0.01$ for Cu water nanofluids. Figure 1 shows the variations of permeability of porous medium and Casson parameter on primary velocity. It is clear that the primary vel0city decreases with the increase in porous medium parameter of the fluid due to enhancement of the viscosity of fluid or decrease in the stretching rate of the acceleration on the surface and also the primary velocity decreases for the increasing values of Casson parameter. The effect of porous medium and Casson parameter on secondary velocity is displayed in the figure 2. The secondary velocity increases with the increase in porous medium parameter whereas it decreases for the increasing values of Casson parameter. Table 1 illustrates the variations in skin friction coefficient, Nusselt number and Sherwood number for various values of porous medium and Casson parameter.

Figure 3 states the effect of Prandtl number and heat generation parameter on temperature. It is clear that temperature decreases for increased values of Prandtl number. An increase in the Prandtl number reduces the thermal boundary layer thickness. It is seen that an increase in heat generation parameter leads to increase in the temperature. The changes in skin friction coefficient, Nusselt number and Sherwood number for increasing values of Prandtl number is displayed in the table 1. The influence of diffusion thermo effect is depicted in figure 4 and it reveals that temperature grows for enhancing it.

The effect of Schmidt number and chemical reaction parameter on concentration is shown in figure 6. Schmidt number is a dimensionless number defined as the ratio of momentum diffusivity and mass diffusivity. It is clear that the concentration increases with the increase in Schmidt number. The effects of skin friction coefficient, Nusselt number and Sherwood number with the enhancement of Schmidt number are shown in table 1.

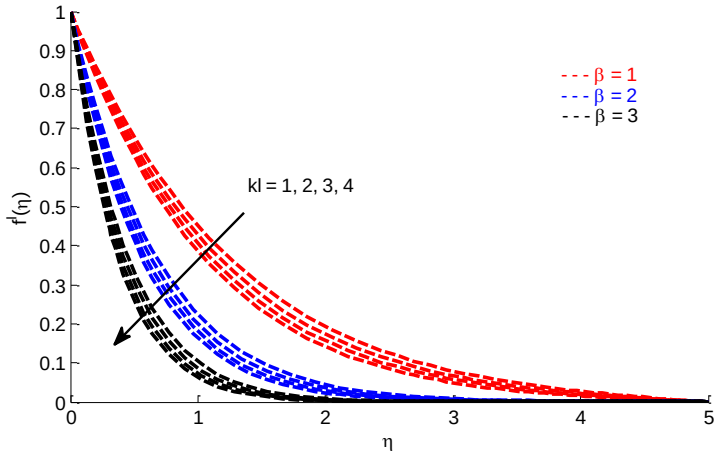

Fig 1**.** Primary velocity profiles for various values of porous medium parameter and casson parameter.

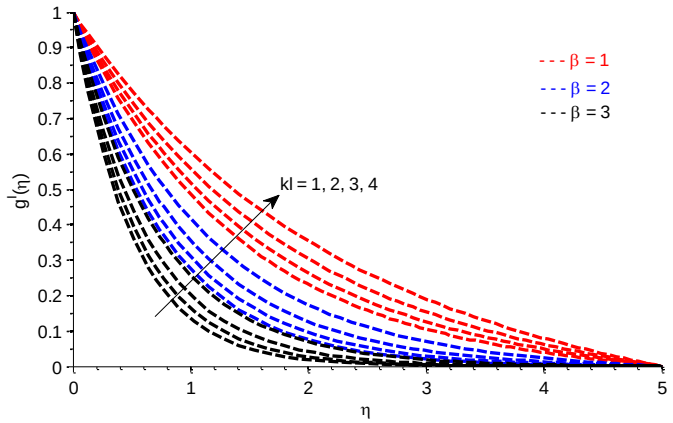

Fig 2**.** Secondary velocity profiles for various values of porous medium parameter and casson parameter.

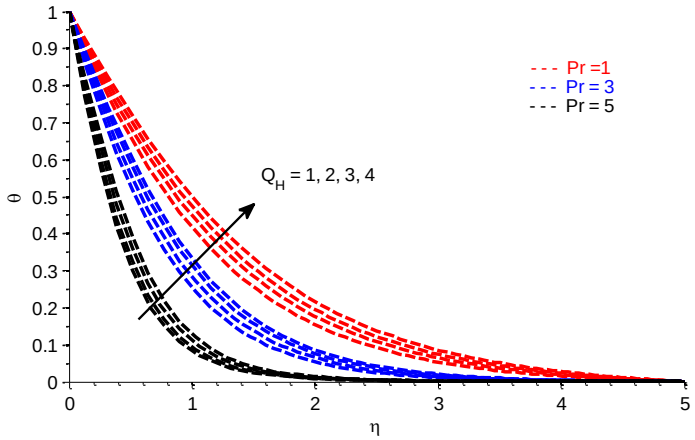

Fig 3**.** Temperature profiles for various values of heat generation parameter and Prandtl number

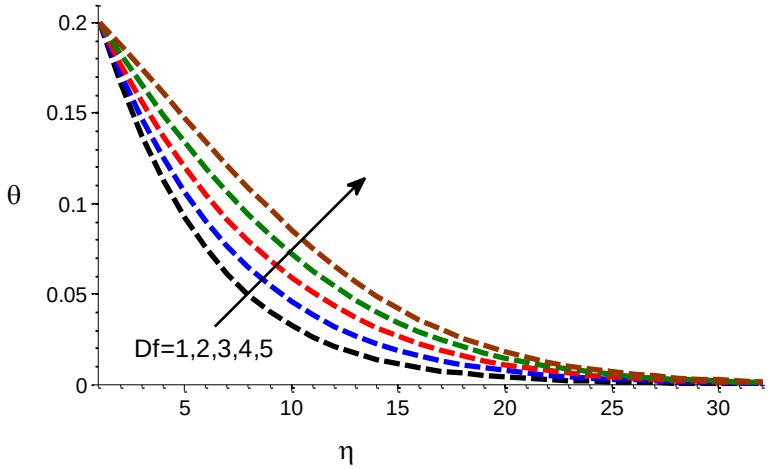

Fig 4. Temperature profiles for various values of Dufour number

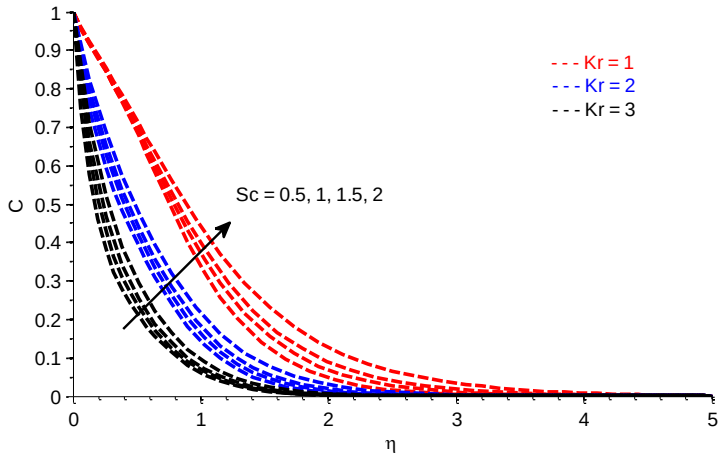

Fig 5. Concentration profiles for various values of Schmidt number and Chemical reaction parameter

Table 1: Skin friction, Nusselt number and Sherwood number under impacts of several terms.

R	Sc	Pr	kl	β	$\mathrm{Re}_x^{\frac{1}{2}} C_{fx}$	$\mathrm{Re}_x^{\frac{1}{2}} C_{fy}$	$\mathrm{Re}_x^{-\frac{1}{2}} Nu_x$	$\mathrm{Re}_x^{-\frac{1}{2}} Sh_x$
0.10	0.10	6.72	1.00	0.10	5.140155	-9.273021	0.010721	1.493261
0.20	0.10	6.72	1.00	0.10	5.146229	-9.271025	0.047918	1.600940
0.10	0.100	6.72	1.00	0.10	8.280679	-9.454326	-0.726268	0.547785
0.10	0.200	6.72	1.00	0.10	7.337017	-9.403679	-0.509991	0.753136
0.10	0.300	6.72	1.00	0.10	6.682429	-9.367103	-0.358259	0.920441
0.10	0.10	5.00	1.00	0.10	5.511043	-9.265077	1.638921	6.807938
0.10	0.10	6.72	1.00	0.10	5.590133	-9.267227	2.142166	8.698359
0.10	0.10	6.72	0.10	0.10	8.325454	-9.821725	0.247433	1.378502
0.10	0.10	6.72	0.20	0.10	7.952794	-9.762121	0.220805	1.391476
0.10	0.10	6.72	1.00	0.10	5.140155	-9.273021	0.010721	1.493261
0.10	0.10	6.72	1.00	0.20	2.600976	-6.782319	0.135510	1.435817

3. CONCLUSION

To analyze the flow pattern of Casson nanofluid a numerical study has been performed past a stretched sheet in a conducting field. The governed ordinary differential equations are solved by shooting method using MAT Lab. The concluding points in this study can be noted as follows.

- The primary velocity profile descends for the enhanced values of porous medium parameter and Casson parameter.
- The secondary velocity profiles enhances under the increment of porous values whereas it decline with the enhancement of Casson parameter.
- With an increase in Prandtl number, the temperature decreases whereas the temperature increases for the increasing values of heat generation parameter.

- The concentration profiles enhances with the enhancement of Schmidt parameter.

4. REFERENCES:

1. Choi S.U.S, Enhancing Thermal Conductivity of Fluids with Nanoparticles, Developments and Applications of Non-Newtonian Flows. FED-231/MD-vol (66) (1995) 99–1053.
2. Choi, S.U.S., Zhang, Z. G., Yu, W., Lockwood, F. E., Grulke, E. A., Anomalous Thermal Conductivity Enhancement in Nanotube Suspensions, Applied Physics Letters, 79 (2001) 2252.
3. Hamad M.A.A.,Analytical Solution of Natural Convection Flow of a Nanofluid over a linearly Stretching Sheet in the Presence of Magnetic Field, International Communications in Heat and Mass Transfer, 38(4) (2011) 487-492.
4. Khan M. S., Alam M. M., Ferdows M, Effects of Magnetic Field on Radiative Flow of a Nanofluid Past a Stretching Sheet, Procedia Engineering, 56 (2013) 316-322.
5. Nayak M.K., Akbar N.S., Tripathi D., Pandey V.S., Three Dimensional MHD Flow of Nanofluid over an Exponential Porous Stretching Sheet with Convective Boundary Conditions, Thermal Science and Engineering Progress, 3 (2017) 133-140.
6. Hayat, T., Muhammad, T., Shehzad, S.A., and Alsaedi, A., Soret and Dufour Effects in Three-dimensional Flow over an Exponentially Stretching Surface with Porous Medium, Chemical Reaction And Heat Source/sink, Int. J of Numerical Methods for Heat & Fluid Flow, 25(4) (2015) 762 – 781.
7. Sheikholeslami M, GorjiBandpy M, Ellahi R., Zeeshan A, Simulation of MHD CuO–water Nano fluid Flow and Convective Heat Transfer Considering Lorentz Forces, Journal of Magnetism and Magnetic Materials, 369 (2014) 69-80.
8. Aurang Zaib, et al., Numerical solution of second law analysis for MHD Casson nanofluid past a wedge with activation energy and binary chemical reaction, International Journal of Numerical Methods for Heat & Fluid Flow, 27(12) (2015) 2816–2834.
9. Hayat T, Imtiaz M, Alsaedi A, Mansoor R Magnetohydrodynamic three-dimensional flow of nanofluid by a porous shrinking surface. J. Aerospace Eng. 29(2) (2015).
10. Nayak M .K, Noreen Sher Akbar, Pandey V.S, Zafar Hayat Khan, Dharmendra Tripathi, 3D free convective MHD flow of nanofluid over permeable linear stretching sheet with thermal radiation, Powder Technology. 315 (2017) 205-215.